Journal of Pharmaceutical and Biomedical Analysis 238 (2024) 115862

Contents lists available at ScienceDirect

Journal of Pharmaceutical and Biomedical Analysis

journal homepage: www.journals.elsevier.com/journal-of-pharmaceutical-and-biomedical-analysis

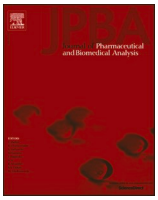

Selective and reliable fluorometric quantitation of anti-cancer drug in real plasma samples using nitrogen-doped carbon dots after MMIPs solid phase microextraction: Monitoring methotrexate plasma level

Ahmed Z. Alanazi [a], Khalid Alhazzani [a], Aya M. Mostafa [b,c], James Barker [b], Mohamed M. El-Wekil [c], Al-Montaser Bellah H. Ali [c,*]

[a] Department of Pharmacology and Toxicology, College of Pharmacy, King Saud University, Riyadh, Saudi Arabia
[b] School of Life Sciences, Pharmacy, and Chemistry, Kingston University, Kingston-upon-Thames, London KT1 2EE, UK
[c] Department of Pharmaceutical Analytical Chemistry, Faculty of Pharmacy, Assiut University, Assiut, Egypt

ARTICLE INFO

Keywords:
Annona squamosal seeds
Magnetic Molecularly-imprinted solid-phase microextraction
Methotrexate
Ratiometric
Plasma

ABSTRACT

A novel selective and reliable ratiometric fluorescence probe has been successfully synthesized for precise, sensitive, and simple quantitation of methotrexate (MTX). Hydrothermal method was employed to fabricate nitrogen-doped carbon dots using *Annona squamosa* seeds (AS-CDs) as a starting material, and their characteristics were confirmed using transmission electron microscopy (TEM), UV-Vis spectroscopy, fluorescence spectroscopy, X-ray diffractometry (XRD), and Fourier Transform Infrared Spectroscopy (FTIR). The ratiometric fluorometric assay, which is based on measuring the ratio of emissions (F_{355}/F_{430}), has a wide detection range of 5–2000 ng /mL and a limit of detection (LOD, S/N = 3) of 1.5 ng /mL. The developed sensing method was successfully applied to the quantification of MTX in rabbit plasma samples and parenteral formulations, achieving satisfactory recoveries %. Magnetic molecularly imprinted solid-phase microextraction was used for selective extraction of MTX from plasma samples. The pharmacokinetic parameters were successfully determined in real rabbit plasma samples after intravenous administration of MTX. The as-designed probe does not only improve the sensitivity, but also enhances the precision and accuracy of the proposed method. Overall, this study presents a promising approach for the detection of MTX in genuine samples with acceptable degree of selectivity and sensitivity.

1. Introduction

Light emissive carbon dots (CDs) have received a significant interest due to their unique properties with a size less than 10 nm. The most intriguing qualities of CDs are water solubility, chemical inertness, photoluminescence, low toxicity, biocompatibility, photostability, ease of functionalization, and low-cost of production [1]. The hydrothermal method is a popular choice for synthesizing CDs due to its simplicity, cost-effectiveness, and ability to provide controlled reaction conditions [2–4]. The derivation of CDs from natural sources, including fruits, vegetables, plants and animal derivatives, has gained significant attention as a research topic [5]. *Annona squamosa* seeds contains a variety of phytoconstituents, which serve as the primary carbon source for synthesizing nitrogen-doped carbon dots (N @ CDs) [6]. The current study involved the production of fluorescent N @ CDs using the hydrothermal method, with *Annona squamosa* seeds (AS- N @ CDs) serving as the primary carbon-rich source for the synthesis process.

Methotrexate (MTX) is a chemotherapeutic agent that serves as a folate antagonist and antimetabolite, and is widely used for the treatment of various types of cancer, including leukemia, osteosarcoma, breast cancer, malignant lymphoma, and other neoplastic disorders. In addition to its anti-tumor properties, MTX also has anti-inflammatory effects and is utilized for treating various conditions such as psoriasis, rheumatoid arthritis, and lupus [7]. The administration of MTX is often accompanied by a range of side effects, including cardio-toxicity, hepatotoxicity, bone marrow suppression, hypo-albuminuria, renal toxicity, pulmonary toxicity, low white blood cell counts, and myelosuppression. As a result, the use of high doses (1 g per vial) of MTX has been limited in clinical applications [8]. MTX has a narrow therapeutic range, and exceeding the recommended dose can have life-threatening

* Corresponding author.
E-mail address: Almontaser_bellah@aun.edu.eg (A.-M.B.H. Ali).

https://doi.org/10.1016/j.jpba.2023.115862
Received 10 September 2023; Received in revised form 27 October 2023; Accepted 9 November 2023
Available online 10 November 2023

consequences [9]. Therapeutic drug monitoring can be a useful tool in ensuring the efficacy and safety of MTX treatment. Therefore, it is crucial to accurately measure MTX concentrations in patients' plasma. Therefore, monitoring the pharmacokinetic parameters of methotrexate is crucial for ensuring the safe and effective use of the drug, as it allows healthcare providers to tailor dosing regimens, minimize toxicity, and optimize therapeutic outcomes.

Molecularly-imprinted polymers (MIPs) are synthetic nanomaterials containing specific recognition sites for the target molecule [10]. These sites are formed by co-polymerizing monomers in the presence of a template molecule that is extracted afterwards, leaving behind complementary cavities [11]. The selectivity and affinity of MIPs make them ideal candidate for sample preparation techniques like solid-phase extraction (SPE) to isolate drugs from complex biological matrices [12]. Key advantages of MIPs include excellent extraction efficiency, ability to isolate drugs from complex matrices, selectivity over metabolites, cost-effectiveness compared to biological binders, physical robustness, and the capacity to be reused [13]. The specificity provided by MIPs provides excellent extraction efficiency and allows accurate quantitation of drugs without interference from metabolites or other sample components [13]. Magnetic molecularly-imprinted solid-phase extraction (MMIP-SPE) is a technique that combines the selectivity of molecularly imprinted polymers (MIPs) with the convenience of magnetic separation [14]. In MMIP-SPE, MIPs are incorporated with magnetic particles, such as iron oxide (Fe_3O_4) nanoparticles [15]. This allows ease and rapid separation of the MIP by applying an external magnetic field. For drugs like MTX with multiple metabolites, MMIP-SPE can play a valuable role in selective sample clean-up prior to analysis. This provides advantages over standard extraction methods and supports the importance of MMIPs as selective sorbents for pharmaceutical and bioanalytical applications [13].

In the original research [16], the efficiency of MTX extraction using MMIP was fine-tuned through a systematic evaluation of various parameters. Increased MIP mass up to 100 mg improved extraction capacity but plateaued at higher amounts. An extraction time of 2 h was optimal for maximizing MTX adsorption. A 20% methanol wash solution achieved the best removal of non-specific matrix components while retaining MTX. Methanol-acetic acid (80:20 v/v) provided the most effective elution solvent, with 5 mL volume needed for complete MTX recovery. Finally, 60 min was sufficient for complete elution. The adsorption experiments revealed that the MMIPs exhibited superior adsorption properties for MTX compared to MNIPs. The static adsorption curves demonstrated that MMIPs had a significantly higher MTX binding capacity, attributed to the presence of imprinted holes on their surface. The dynamic adsorption experiments showed that MMIPs had a faster adsorption rate and stronger adsorption capacity, reaching equilibrium at 60 min. The pseudo-second-order model provided an excellent fit for the adsorption kinetics. Additionally, MMIPs exhibited selective recognition of MTX over its structural analogs, indicating their ability to selectively bind the target molecule.

Herein, we developed a reliable and selective method for detecting MTX levels in plasma by integrating MMIP-SPE with fluorescence detection. This approach simplifies sample pretreatment and reduces interference from proteins and MTX metabolites during analysis. The MMIP-SPE selectively extracts MTX from plasma samples, providing clean extracts for sensitive fluorescence measurement. By combining the selectivity of MMIP-SPE for MTX with the sensitivity of fluorescence detection, this method enables a reliable quantification of MTX in plasma samples with minimal sample preparation and interference. The fluorometric method for detecting MTX is based on using AS-CDs as a ratiometric fluorescence sensor. The ratiometric detection method significantly improved the accuracy and sensitivity of the MTX sensor due to its low background signal. The sensor was found to be effective in detecting MTX in plasma samples and pharmaceutical injections. The fundamental pharmacokinetic parameters were investigated in real rabbit plasma samples.

The developed fluorometric method for determining MTX using AS-CDs surpasses the reported methods using different carbon dots in several key aspects. Firstly, our proposed method incorporates a selective extraction technique using MMIP to isolate MTX from the complex plasma matrix. This approach ensures minimal interference from proteins and other MTX-related metabolites, enhancing the method's accuracy and specificity. Secondly, while previously reported sensors rely on single peak fluorescence emissions, which can be susceptible to interference from varying environmental conditions, our ratiometric method utilizes two distinct wavelengths. This dual-wavelength approach effectively eliminates the potential for interference, enhancing the reliability and robustness of our method, making it a superior choice for accurate MTX quantification in practical applications.

2. Materials and methods

2.1. Reagents and chemicals

The chemicals employed in the experiment were of a high purity suitable for analytical purposes. Methotrexate (MTX) with a purity more than 99% was obtained from Merck (Darmstad, Germany). Quinine sulfate dihydrate, 3-Aminopropyl triethoxysilane (APTES, 98%) and tetraethyl orthosilicate (TEOS, 98%) were supplied by Sigma-Aldrich Co., Ltd., USA. Unitrexate® vial contained 1.0 g MTX per vial and it was bought from a local pharmacy. *Annona squamosa* fruit were purchased from a local market and the seeds were collected from the fruit. Methanol, ammonium hydroxide, potassium hydroxide, ethanol, acetonitrile, $FeCl_3{\cdot}6\ H_2O$, $FeSO_4{\cdot}7\ H_2O$, calcium phosphate, sodium chloride, sodium nitrate, L-arginine, glucose, uric acid, cysteine, glycine, proline, bovine serum albumin, dopamine, tyrosine and folic acid were provided by Fluka (Buchs, Switzerland). Dihydrogen sodium phosphate and hydrogen disodium phosphate were purchased from Merck (Cairo, Egypt). All solutions were prepared using double-distilled water.

2.2. Instrumentation

Absorption spectra were recorded on a double-beam UV1601 PC Ultraviolet–visible spectrophotometer (Shimadzu, Tokyo, Japan) with a cuvette with a 1 cm optical path. Fluorescence spectra were recorded on a RF-5301PC Shimadzu fluorescence spectrophotometer (Tokyo, Japan) equipped with a xenon lamp and quartz cell with excitation and emission slit at 5 nm. The Fourier-transform infrared (FT-IR) spectra of AS-CDs were recorded on a Nicolet 6700 instrument (Thermo Electron Corporation, USA) at scanning range from 4000 to 400 cm^{-1}. The X-ray diffraction (XRD) pattern was performed using Philips PW 1700 X-Ray diffractometer (Eindhoven, Netherlands). The morphological evaluation of AS-CDs was studied by transmission electron microscope (TEM) (JEOL, JEM-1400, 200 kv, Japan). X-ray photoelectron spectrometer (XPS, ESCA Ulvac-PHI 1600, PHI Quantum 2000 XPS system, Physical Electronics, USA) was used to reveal the surface functional groups of AS-CDs.

2.3. Synthesis of AS-CDs

The *Annona squamosa* fruits were thoroughly cleansed multiple times with double distilled water to remove any contaminants before being sliced into small pieces, and the fruits were peeled to obtain seeds. The seeds were then dried under sunlight. A quantity of 0.5 g of dried *Annona squamosa* seeds was ground into powder using a mortar and pestle and sifted through an 80-mesh standard sieve. After that, the seed powder was subjected to ultrasonication in a beaker along with 20 mL of double distilled water for 20 min. The resulting mixture was then poured into a 50 mL Teflon-coated stainless steel pressure vessel and heated to 200 °C under pressure for 6 h. After the temperature of the solution had fallen to around that of the surrounding environment, the resulting yellow

product was collected and any large particles were removed by centrifugation for 3 min at 4000 rpm. The solutions were then passed through a 0.22 μm syringe filter to eliminate any remaining microparticles. Finally, the yellow AS-CDs solutions were stored at 4 °C for future use.

2.4. Sample pretreatment and extraction

2.4.1. Preparation of magnetic nanoparticles coated by silica (Fe_3O_4 @SiO_2 MNPs)

Fe_3O_4 @SiO_2 was synthesized following established procedure [17]. The reported procedures are mentioned in supplementary data file.

2.4.2. Preparation of MMIPs and MNIPs

MMIPs were synthesized using a procedure previously reported [16]. The reported procedures are mentioned in the supplementary data file.

2.4.3. MMIPs-SPE procedure

MMIPs-SPE procedure of MTX in biological fluids were previously reported [16]. The plasma sample (500 μL) was spiked with known concentrations of MTX (500 μg /mL) standard in 5 mL heparinized tubes. To precipitate plasma proteins, 500 μL of acetonitrile was added to each tube, followed by vortex mixing for 5 min and centrifugation at 8000 rpm for 5 min. The resulting supernatants were quantitatively transferred to 5 mL volumetric flask. For the extraction, 100 mg of MMIPs were first activated by shaking in 10 mL of methanol for 5 min and separated magnetically. The content of 5 mL volumetric flask was then added to the activated MMIPs and extracted by shaking for 240 min at room temperature. Elution of MTX was performed by adding 5 mL of methanol-acetic acid solution (4:1 v/v) and shaking for 60 min. The eluent was collected in test tubes, dried under nitrogen, and completed to 700 μL with methanol for subsequent fluorescence analysis to quantitate MTX levels.

2.5. Procedures for ratiometric fluorescence determination of MTX

A solution containing 300 μL of AS-CDs, 2.0 mL of a phosphate buffer solution (pH 7.0), and 700 μL of different concentrations of MTX was prepared. The mixture was then incubated for 1 min before dilution with methanol to achieve a final volume of 5.0 mL. Next, fluorescence spectra were collected in the 300–600 nm wavelength range with excitation at 300 nm. The fluorescence intensity ratio was measured with varying MTX concentrations at emission wavelengths of 355 nm (Native fluorescence of MTX) and at 430 nm (Fluorescence of AS-CDs) to determine the MTX concentration.

2.6. Pharmacokinetic application

A pharmacokinetic study was conducted on six healthy male New Zealand rabbits weighing 2.0–2.5 Kg to investigate the pharmacokinetics of MTX. The rabbits were given time to adapt to standard laboratory conditions for two weeks, which included a 12-hour light/dark cycle, a temperature of 25 ± 5 °C, and unrestricted access to food and water. The study protocol was approved by the ethics committee at Assiut University (06/2023/0133), Egypt, and adhered to the guidelines of the Declaration of Helsinki. Intravenous bolus injection of MTX at a dose of 15.0 mg/kg was given through the marginal ear vein of rabbits. Food intake was restricted after the dose, while water was provided without restriction. Blood samples for pharmacokinetic analysis were collected at various time points: at 0.25, 0.5, 1, 1.5, 2, 4, 6, 10, and 12-h post-dose. Each sample (1.0 mL) was collected in heparinized tubes. Following collection, the plasma was separated by centrifugation at 5000 rpm for 5 min at a temperature of 5 °C, and subsequently stored at − 20 °C until further analysis.

2.7. Analysis of MTX in parenteral formulation

The MTX quantification method developed in this study was tested on a parenteral formulation (1.0 g/ vial, Unitrexate® vial). To determine the MTX concentration, the samples were diluted with methanol to achieve a final concentration range of 5.0–2000 ng /mL.

3. Results and discussion

3.1. Morphological and spectroscopic characterization of AS-CDs

TEM measurement was conducted to verify the size and morphology of AS-CDs. By analyzing the TEM image, it showed that AS-CDs has a spherical shape and well dispersion with diameters of approximately 3–4 nm as can be seen in Fig. 1 A and the particle size distribution histogram (Fig. 1 A inset). The XRD pattern of the AS-CDs shows a broad diffraction peak at 24.9° and this pattern revealed the amorphous surface of AS-CDs (Fig. 1B) [18]. Fig. 1 C was obtained after performing FTIR measurements in order to gain a deeper understanding of the functional groups present on the surface of the AS-CDs. The broad absorption band observed around 3405 cm^{-1} was determined to be associated with the stretching vibration of N–H/O–H [19]. In addition, the spectrum showed stretching vibrations of C-H at 2924 and 2851 cm^{-1}. The typical range for the C-O stretching vibration on the aromatic ring was found to be between 1031 and 1110 cm^{-1} [20]. The stretching vibrations of C═O and C-N were linked to the notable absorption peaks detected at approximately 1658 cm^{-1} and 1433 cm^{-1}, respectively. Furthermore, the bending vibration of C-H was associated with the absorption band at 610 cm^{-1} [21]. The FTIR spectrum of AS-CDs indicated the presence of various functional groups on their surface, including amino, acidic, hydroxyl, and carbonyl moieties. The broad band observed at 3405 cm^{-1} was attributed to the presence of –OH/–NH functional groups or hetero atom doping, indicating the likely presence of nitrogen in the AS-CDs. The XPS survey revealed that the as-synthesized AS-CDs have typical signals of C 1 s, N 1 s, and O 1 s with binding energies of 289 eV, 400 eV, and 537 eV, respectively (Fig. S1) [22].

3.2. Optical characterization of AS-CDs

The UV–vis absorption spectrum of the AS-CDs displayed a weak band at 280 nm, which is attributed to the π-π * transition of the C═C group. Additionally, a noticeable absorption peak was observed at 350 nm, which was assigned to the n-π * transition of the C═O/C═N bonds [19,20]. The AS-CDs demonstrated distinct and intense fluorescence with highest emission at 430 nm when excited at 320 nm, as depicted in Fig. 2A. Furthermore, their fluorescence properties were dependent on the excitation wavelength, as shown in Fig. 2B when they were excited from 300 nm to 400 nm. The quantum yield of AS-CDs was determined to be 36.5% by comparing it to the reference quantum yield of 54% obtained using quinine sulfate in 0.1 mol/L H_2SO_4. This calculation involved measuring the absorbance and emission spectra of AS-CDs and quinine sulfate at 360 nm excitation wavelength and substituting the absorbance and fluorescence integral area into a formula [23]:

$$\phi_{AS-CDs} = \phi_{QS} \times \frac{F_{AS-CDs}}{F_{QS}} \times \frac{A_{QS}}{A_{AS-CDs}} \times \frac{\eta_{AS-CDs}}{\eta_{QS}}$$

The quantum yield of AS-CDs is represented by $\phi_{AS\text{-}CDs}$, while ϕ_{QS} represents the quantum yield of QS. $F_{AS\text{-}CDs}$ indicates the fluorescence intensity of AS-CDs, and F_{QS} corresponds to the fluorescence intensity of quinine sulfate. **A** represents the absorbance value, and η denotes the refractive index of the solvent. For the AS-CDs, the solvent used was distilled water with a refractive index of 1.33, while for quinine sulfate; it was 0.1 M H_2SO_4 with a refractive index of 1.33.

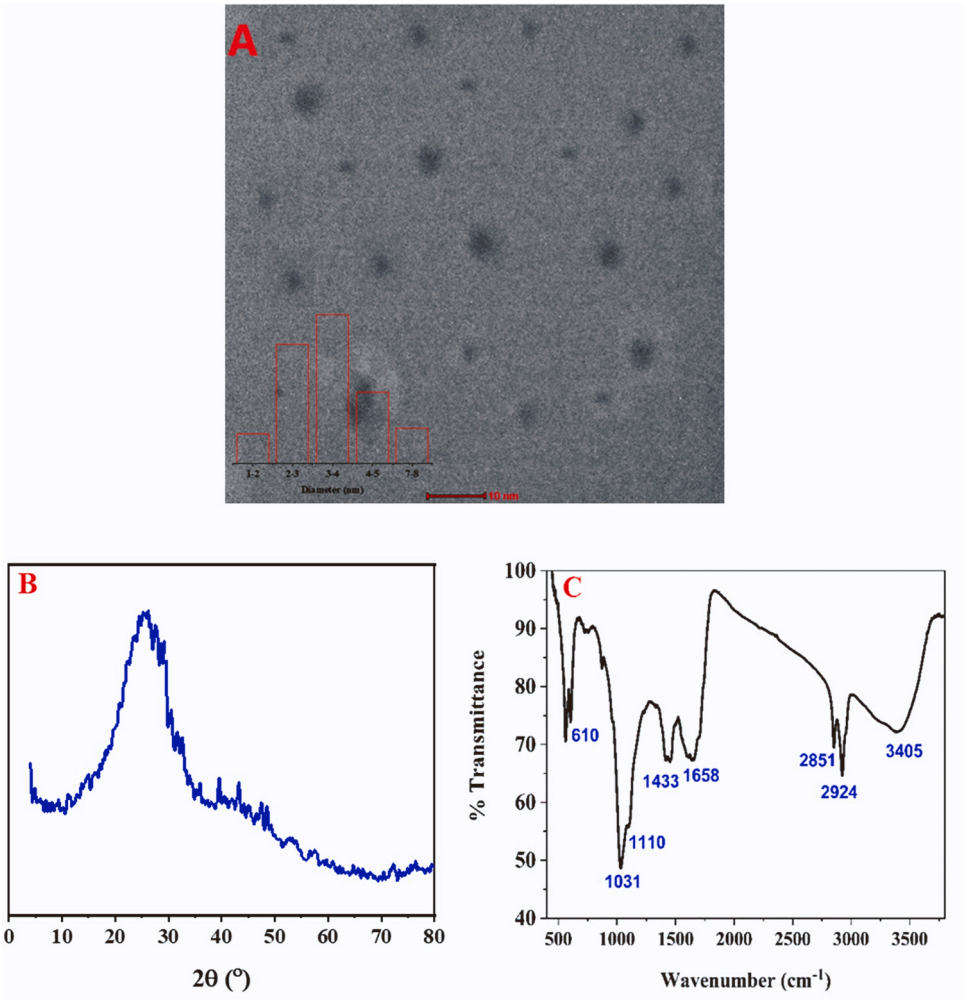

Fig. 1. (A) TEM image (inset: size distribution histogram), (B) XRD and (C) FT-IR characterization of the produced AS-CDs.

3.3. Stability of AS-CDs

To ensure the stability of AS-CDs as a fluorescent probe, their fluorescence performance was tested under different conditions. The results, illustrated in Fig. S2A, demonstrate an increase in emission intensity at 430 nm as the pH value increased, with the fluorescence remaining relatively stable after reaching a pH of 5. These findings suggest that AS-CDs are not stable in a highly acidic range of pH values and have the potential to be used in applications that require neutral or alkaline medium. This may be attributed to the aggregation-induced quenching occurred in high acidic medium (pH 1–3) [24]. Fig. S2B demonstrates that the fluorescence intensities of AS-CDs remain relatively stable even at NaCl concentrations as high as 1.0 M, indicating the excellent salt tolerance. To evaluate the photostability of AS-CDs, fluorescence spectra were recorded under a 365 nm UV lamp at various exposure times ranging from 0 to 10.0 h. As shown in Fig. S2C, no significant changes in fluorescence were observed during this period, indicating that AS-CDs exhibit excellent resistance to photobleaching and are highly stable.

3.4. Optimization of experimental conditions

To enhance the fluorescence sensitivity of AS-CDs probe, the detection conditions were adjusted. The fluorescence intensity ratio F_{355}/F_{430} was used as the standard to optimize the experimental conditions including pH, incubation time, volume of AS-CDs and excitation wavelength for the ratiometric determination of MTX and AS-CDs. I_{355} and I_{430} were the fluorescence intensity at 355 nm for MTX and 430 nm for AS-CDs, respectively. The influence of pH in the range of 3–10 was examined (Fig. S3A). The optimal pH for achieving maximum F_{355}/F_{430} ratio is approximately 7. As a final parameter, the volume of AS-CDs introduced into the reaction solution was evaluated. From 100–500 μL of AS-CDs, appropriate ratio intensities (F_{355}/F_{430}) were noted as the volume is 300 μL (Fig. S3B). To determine the optimal reaction time, the effect of reaction time was evaluated over 300 s. The results, as illustrated in Fig. S3C, demonstrated that the highest fluorescence intensity ratio F_{355}/F_{430} was observed after 60 s, indicating that a reaction time of 60 s was optimal for the experiment.

The choice of excitation wavelength is a critical factor in the ratiometric analysis of MTX and AS-CDs due to the potential for interference between their respective emissions. In this study, an excitation wavelength of 300 nm was chosen for MTX because its native emission appears at 355 nm, which does not interfere with the emission wavelength of AS-CDs (Fig. 3). On the other hand, if an excitation wavelength of 350 nm was used, it would result in an native emission at 460 nm that overlaps with the AS-CDs emission at 430 nm, leading to spectral interference and potentially inaccurate results (Fig. 3). However, it should be noted that at 320 nm (the optimum excitation wavelength of AS-CDs), the fluorescence intensity of MTX was considerably lower. Thus, 300 nm was ultimately chosen as the excitation wavelength for both MTX and AS-CDs, as it provided the optimal sensitivity for MTX, and the fluorescence of AS-CDs was only slightly affected.

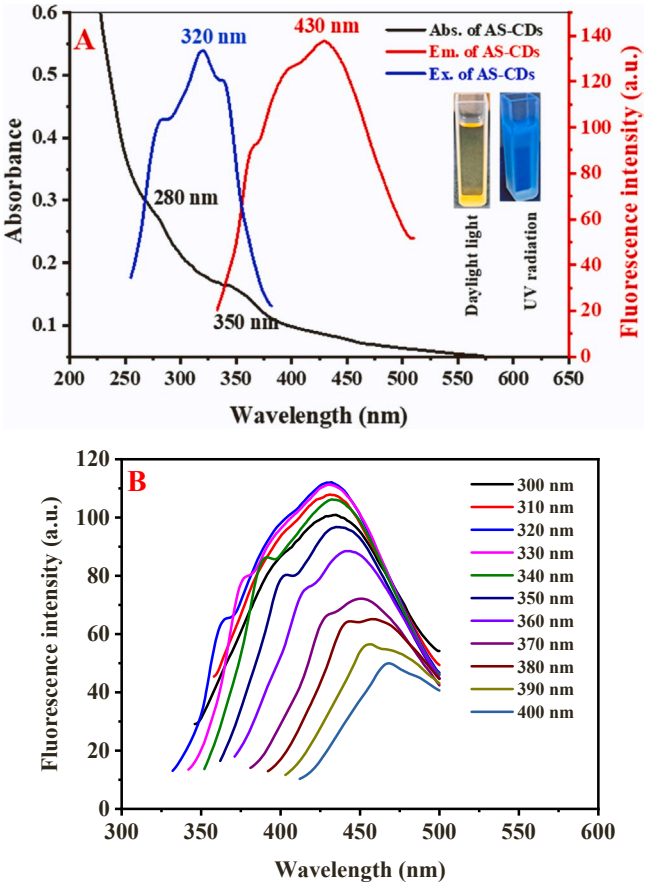

Fig. 2. (A) Overlay of UV–visible absorption spectra, excitation spectra and emission spectra of the AS-CDs solution, Inset: the images of the AS-CDs solution under visible light and UV light at 365 nm. (B) The fluorescence emission spectra of AS-CDs at different excitation wavelengths (from 300–400 nm).

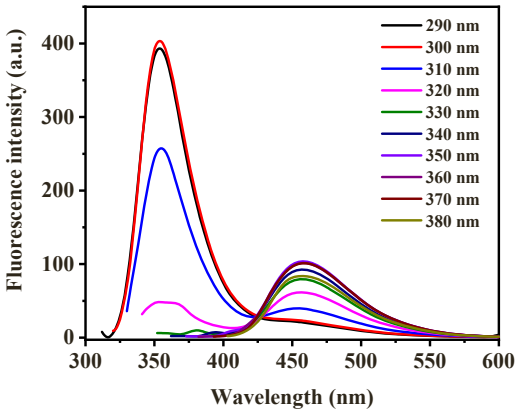

Fig. 3. The fluorescence emission spectra of MTX at different excitation wavelengths (from 290–380 nm).

3.5. Determination of MTX by ratiometric fluorescent probe

The validation of the proposed method was conducted in accordance with the guidelines outlined in ICH Q2 (R1). Under the optimal experimental conditions, the fluorescence of AS-CDs was tested with the gradual addition of MTX, resulting in a decline in fluorescence intensity at 430 nm and an increase at 355 nm. The recorded values of F_{355}/F_{430} demonstrated excellent linearity across the range of MTX concentrations from 5.0–2000 ng /mL, as presented in Fig. 4A and 4B. The linear

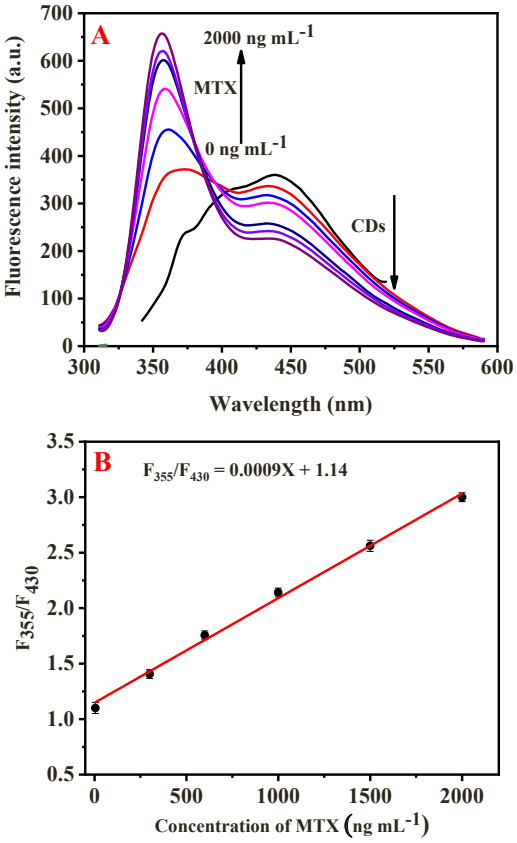

Fig. 4. (A) Fluorescence emission spectrum of AS-CDs after adding different MTX concentration (5.0–2000.0 ng /mL) at λ_{ex} of 320 nm. (B) Plot of (F_{355}/F_{430}) versus MTX concentrations.

regression equation was estimated to be $F_{355}/F_{430} = 0.0009 \cdot C_{MTX} + 1.14$ ($R^2 = 0.9986$). The detection limit (LOD, S/N = 3) was calculated to be 1.46 ng /mL utilizing the formula LOD = 3σ/k, where σ represented the standard deviation of the signal obtained from 10 blank parallel measurements and the calibration curve's slope was denoted by the variable k. To evaluate the precision of the developed method, intra-day precision was assessed by measuring six replicates at three different concentration levels spanning the low, medium, and high ranges of the calibration curve. Inter-day precision, on the other hand, was evaluated over a period of three consecutive days. The precision of the method was expressed as the percent relative standard deviation (% RSD), and the results can be found in Table S1. It is noteworthy that the % RSD values did not exceed 3.81%, indicating that the developed method exhibits satisfactory precision.

The detection performance of MTX was compared with other fluorometric methods and presented in Table 1. The comprehensive evaluation of the comparative data presented in the table justifies the significance of the current work. The proposed method demonstrates several advantages over existing methods. Firstly, it offers higher sensitivity compared to most methods and wider linearity ranges, indicating its ability to detect lower concentrations of the target analyte and cover a broader range of concentrations. Secondly, it stands out as the only method based on ratiometric sensing, which enhances accuracy and reliability by measuring multiple signals simultaneously. This distinguishes it from other methods relying on single-signal measurements. Lastly, the method for preparing the carbon dots used in this work is simpler compared to other fluorescent probes, making it more accessible and practical for potential applications.

The study assessed the regeneration capabilities of MMIPs. In the initial experiment, a sample recovery rate of 98.50% was achieved. Subsequently, in a second extraction experiment conducted under

Table 1
Comparison of different fluorometric methods for MTX detection with the proposed ratiometric method.

Sensors	Mode	Linear range (ng /mL)	LOD (ng /mL)	Ref.
N, S co-doped CDs	Single-signal	0.45–22750	0.15	[25]
Au nanocluster	Single-signal	1.6–24000	0.9	[26]
N, S co-doped CDs	Single-signal	400 - 41300	12	[27]
N, S, P, B co-doped CDs	Single-signal	75–99900	74.9	[28]
N, S co-doped CDs	Single-signal	1330–53400	432.25	[29]
Tb^{3+}-1,10-phenanthroline complex.	Single-signal	20–10000	15	[30]
Terbium-doped dendritic silica particles	Single-signal	100–1000	52.78	[31]
Amine- silica CDs	Single-signal	10–50000	10.0	[32]
AS-CDs	**Ratiometric**	**5 – 2000**	**1.46**	**This work**

identical conditions, the recovery rate was 94.26%. This indicates that the extraction agent developed in this research exhibited a robust regeneration performance, with only a minimal 4.24% decrease in recovery rate after two repeated uses.

3.6. Fluorescence detection mechanism

Fluorescence quenching can occur through static or dynamic mechanisms and can involve various processes such as inner filter effect (IFE), Förster resonance energy transfer (FRET), and photo-induced electron transfer (PET). The UV–vis absorption spectrum of MTX shows absorption peaks at 200–500 nm, with clear UV peaks at 262, 295, and 376 nm. The AS-CDs displayed a well-defined fluorescence emission peak at 430 nm when excited at 300 nm. There was significant overlap between the fluorescence excitation and emission spectra of the AS-CDs and the UV–vis absorption spectrum of MTX (Fig. 5A). Based on these findings, the fluorescence quenching of AS-CDs by MTX might be caused by the IFE or the FRET. In order to verify that the observed fluorescence changes were either due to FRET or IFE, the fluorescence lifetimes of AS-CDs were measured with and without MTX as shown in Fig. 5B. The lifetime of AS-CDs does not change after the addition of MTX. Since the IFE process does not affect the lifetime of AS-CDs, these results indicate the possibility of IFE between AS-CDs and MTX. Therefore, it can be concluded that IFE was the primary cause of the observed fluorescence changes in AS-CDs. To gain a deeper understanding of the quenching mechanism, As shown in Fig. 5C, increasing the temperature resulted in decreasing the slope (K_{sv}) of the Stern-Volmer equation. The Stern-Volmer equation can be represented as follows [33]:

$$F_0/F = 1 + K_{sv}[Q]$$

The fluorescence of AS-CDs in the absence and presence of MTX can be described by F_0, F, and [Q] is the concentration of MTX, while K_{sv} represents the Stern-Volmer constant. The observed decrease in K_{sv} with rising temperature suggests that static quenching dominates the reaction process.

In order to confirm the reduction in fluorescence due to IFE, the Parker Eqs. (1), (2), and (3) were utilized for additional validation [34].

$$\frac{F_{cor}}{F_{obs}} = \frac{2.3dA_{ex}}{1-10^{-dA_{ex}}}10^{gA_{em}} \quad \frac{2.3sA_{em}}{1-10^{-sA_{em}}} \tag{1}$$

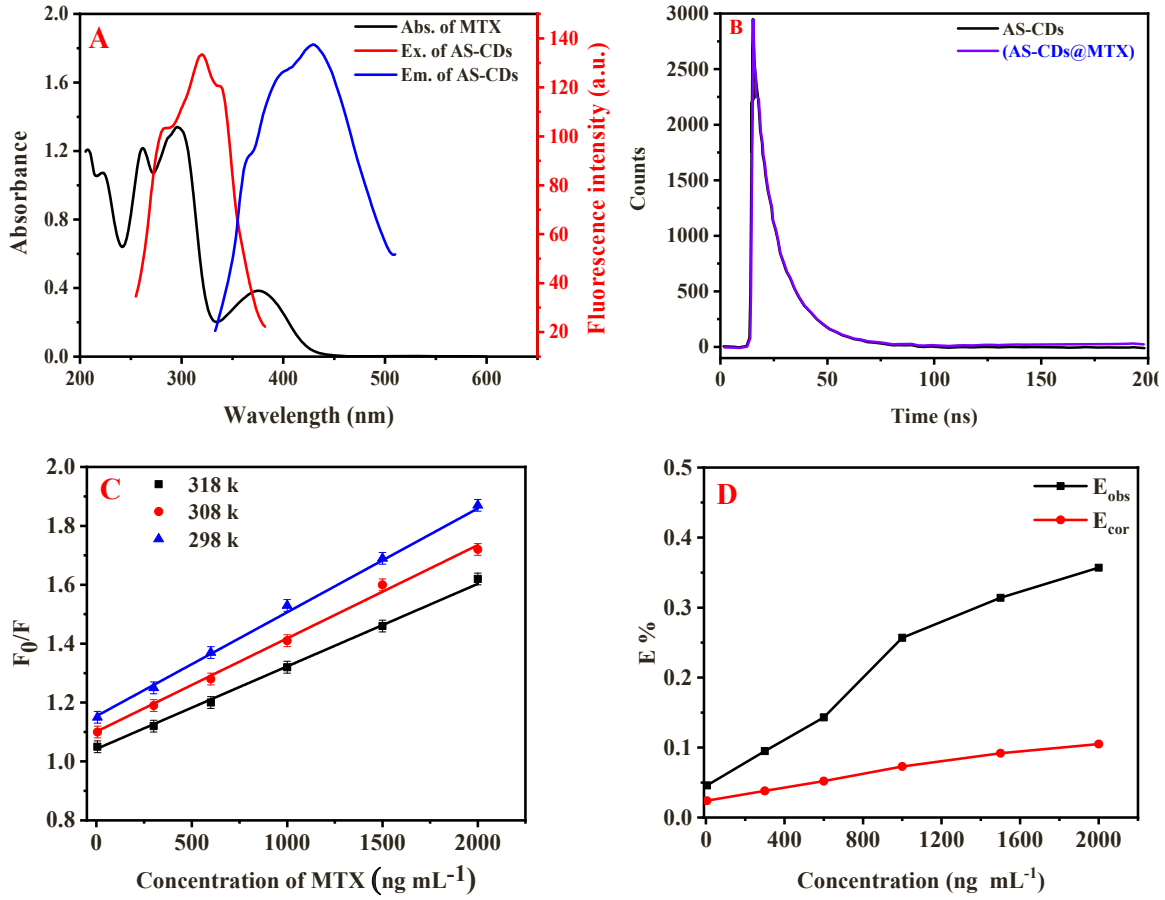

Fig. 5. (A) Fluorescence emission spectra overlap of AS-CDs and UV–vis absorption spectra of MTX (1.0 μg /mL) (B) Fluorescence decay curve of AS-CDs in the absence and presence of MTX, (C) Stern-Volmer plots of AS-CDs (1.0 mg /mL) with MTX (5.0–2000.0 ng /mL) under different temperatures, (D) Suppressed efficiency (E, %) of observed (E_{obs}) and corrected (E_{cor}) fluorescence intensity.

$$E_{obs} = 1 - \frac{F_{obs}}{F_{obs,o}} \quad (2)$$

$$E_{cor} = 1 - \frac{F_{cor}}{F_{cor,o}} \quad (3)$$

F_{obs} represents the observed fluorescence intensity, while F_{cor} denotes the fluorescence intensity after IFE correction. A_{ex} and A_{em} correspond to the absorbance values at 300 and 430 nm, respectively. The parameter 'g' signifies a distance of 0.40 cm, indicating the space between the excitation beam's edge and the cuvette's edge. 's' denotes the thickness of the excitation beam, which is 0.10 cm, and 'd' represents the optical path length of light within the solution, equal to 1.0 cm. F_{obs} and $F_{obs,0}$ represented the fluorescence intensities detected in the presence and absence of MTX, respectively. Similarly, F_{cor} and $F_{cor,0}$ indicated the fluorescence intensities after correction for IFE, with and without MTX. The relevant parameters were computed and presented in Table S2. As indicated in Table S2 and Fig. 5D, as the MTX concentrations increased, both the F_{cor}/F_{obs} ratio and the degree of suppression in the observed fluorescence (E_{obs}) increased. Notably, the E_{obs} value surpassed the E_{cor} value. These experimental findings strongly suggested that the quenching mechanism involved was indeed IFE.

3.7. Selectivity of AS-CDs

In order to assess the selectivity of the AS-CDs sensing probe, we conducted experiments using the developed sensing probe to detect MTX in the presence of a variety of potential interfering agents commonly found in biological matrices. These interfering agents include Ca^{2+}, Mg^{2+}, Al^{3+}, Zn^{2+}, Na^{+}, Fe^{2+}, K^{+}, Cu^{2+}, Co^{2+}, Ni^{2+}, and Fe^{3+}, as well as phosphate, chloride, nitrate, L-arginine, glucose, uric acid, cysteine, glycine, proline, bovine serum albumin, dopamine, tyrosine, and folic acid. The aim was to determine whether the AS-CDs sensing probe was specific to MTX or whether it could be influenced by other potential interfering agents. To assess the selectivity of the probe in plasma matrices, the tolerance limits (The concentration ratio of interfering species to analyte that generates <5% relative error in method sensitivity was determined as the threshold) were calculated (Table S3). These findings suggest that the AS-CDs sensing probe is highly selective and suitable for accurate detection of MTX in the presence of potential interfering agents in plasma samples.

3.8. Analytical applications to plasma samples and injection solution

In order to confirm the suitability of the AS-CDs fluorescent sensor for detecting MTX, we utilized the developed probe to analyze MTX in spiked rabbit plasma samples and injection formulations. The results of these analyses are presented in Table 2, and indicate that the recovery percentages for the selected concentrations fall within acceptable ranges. This suggests that the designed probe has a strong affinity for MTX and is a reliable tool for its detection.

Table 2
Recovery of MTX in plasma samples and parenteral formulations (n = 5).

Added (ng /mL)	Plasma		Parenteral	
	Found (ng /mL)	Recovery (%) ± RSD (%)	Found (ng /mL)	Recovery (%) ± RSD (%)
5	4.90	98.0 ± 1.49	4.92	98.40 ± 1.78
100	97.8	97.80 ± 1.28	98.2	98.20 ± 1.49
600	593	98.83 ± 1.84	595	99.17 ± 2.53
1000	989	98.90 ± 2.01	992	99.20 ± 2.41

3.9. Pharmacokinetic applications

The validated method was successfully employed to quantify the concentrations of MTX in rabbit plasma. Fig. 6 illustrates the mean concentration-time curves of MTX in rabbit plasma following a single intravenous bolus administration of 15 mg/kg. Table 3 presents the main pharmacokinetic parameters. The maximum (C_{max}) and minimum (C_{min}) plasma concentrations observed in the pharmacokinetic study samples were within the calibration range of the validated methods. MTX pharmacokinetics after intravenous administration generally follows a two-compartment model.

4. Conclusion (s)

To summarize, we have developed a highly selective ratiometric fluorescence probe, utilizing blue emissive fluorescent carbon dots derived from *Annona squamosa* seeds (AS-CDs), for the detection of MTX. Upon addition of MTX, the fluorescence of the AS-CDs at 430 nm is quenched, while the fluorescence of MTX is increased at 355 nm. This ratiometric method for MTX detection offers a more precise measurement by detecting changes in the ratio of fluorescence intensities. Our designed probe has been successfully used for MTX determination with a low detection limit (1.46 ng /mL), good selectivity, and competitive detection speed. Moreover, we have applied this method for the detection of MTX in rabbit plasma, which is of biological significance, as MTX has a narrow therapeutic index. The sources of errors in this study include the non-specific adsorption of interferents on the surface of MMIPs particles, which can be suppressed using differential study. Moreover, the influence of the primary IFE on the ratiometric fluorescence intensity can be corrected according to the absorbance readout, which is beneficial to enhance the anti-interference ability of the fluorometry [35]. Our developed ratiometric probe holds promise for monitoring pharmacokinetic parameters of MTX in real plasma samples, and offers improved accuracy and sensitivity for the detection of MTX.

CRediT authorship contribution statement

Dr. Ahmed Z. Alanazi: Conceptualization, Funding acquisition, Investigation, Methodology, Project administration, Resources, Validation, Writing – review & editing. **Dr. Khalid Alhazzani:** Conceptualization, Funding acquisition, Investigation, Methodology, Project administration, Resources, Validation, Writing – review & editing. **Dr. Aya M. Mostafa:** Conceptualization, Funding acquisition, Investigation, Methodology, Project administration, Resources, Validation, Writing – review & editing. **Dr. James Barker:** Conceptualization, Funding acquisition, Investigation, Methodology, Project administration, Resources, Validation, Writing – review & editing. **Dr. Mohamed M. El-**

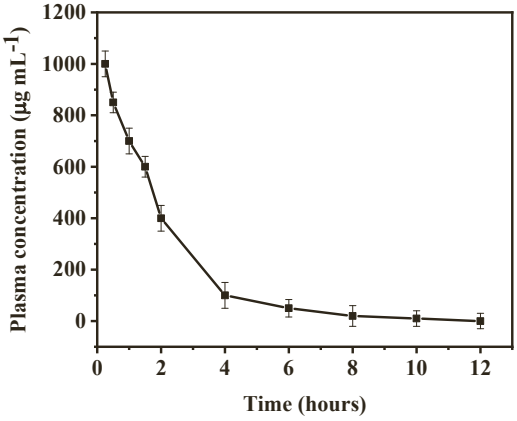

Fig. 6. Plasma pharmacokinetic profile after I.V. bolus injection of MTX in rabbits (15 mg/kg).

Table 3
Pharmacokinetics of MTX following intravenous bolus administration in rabbits (n = 6).

Parameters	MTX
C_{max} (μg /mL)	998±81.25
$t_{1/2}\alpha$ (h)	0.22±0.052
$t_{1/2}\beta$ (h)	2.5±0.73
V_c (L /kg)	0.03±0.014
V_p (L /kg)	0.08±0.034
k_{el} (h^{-1})	0.28±0.024
CL (L /kg′h)	0.046±0.011
MRT (h)	4.5±0.89
AUC_{0-12} (μg hr /mL)	4500 ± 963.42
$AUC_{0-\infty}$ (μg hr /mL)	650± 952.50

Wekil: Conceptualization, Funding acquisition, Investigation, Methodology, Project administration, Resources, Validation, Writing – review & editing. **Dr. Al-Montaser Bellah H. Ali:** Conceptualization, Funding acquisition, Investigation, Methodology, Project administration, Resources, Validation, Writing – review & editing.

Declaration of Competing Interest

The authors declare that they have no known competing financial interests or personal relationships that could have appeared to influence the work reported in this paper.

Acknowledgements

The authors would like to extend their appreciation to the Researchers Supporting Project number (RSPD2023R563) at King Saud University, Riyadh, Saudi Arabia.

Appendix A. Supporting information

Supplementary data associated with this article can be found in the online version at doi:10.1016/j.jpba.2023.115862.

References

[1] S.N. Baker, G.A. Baker, Luminescent carbon nanodots: emergent nanolights, Angew. Chem. Int. Ed. 49 (38) (2010) 6726–6744.
[2] M. Bazargan, F. Ghaemi, A. Amiri, M. Mirzaei, Metal–organic framework-based sorbents in analytical sample preparation, Coord. Chem. Rev. 445 (2021), 214107.
[3] E. Torabi, M. Mirzaei, M. Bazargan, A. Amiri, A critical review of covalent organic frameworks-based sorbents in extraction methods, Anal. Chim. Acta 1224 (2022), 340207.
[4] E. Torabi, M. Moghadasi, M. Mirzaei, A. Amiri, Nanofiber-based sorbents: Current status and applications in extraction methods, J. Chromatogr. A. 2023 (1689), 463739.
[5] C. Kang, Y. Huang, H. Yang, X.F. Yan, Z.P. Chen, A review of carbon dots produced from biomass wastes, Nanomaterials 10 (2020) 2316.
[6] G. Madhumitha, G. Rajakumar, S.M. Roopan, A.A. Rahuman, K.M. Priya, A. M. Saral, F.R.N. Khan, V.G. Khanna, K. Velayutham, C. Jayaseelan, Acaricidal, insecticidal, and larvicidal efficacy of fruit peel aqueous extract of Annona squamosa and its compounds against blood-feeding parasites, Parasitol. Res. 111 (2012) 2189–2199.
[7] M.F. Silva, C. Ribeiro, V.M. Gonçalves, M.E. Tiritan, Á. Lima, Liquid chromatographic methods for the therapeutic drug monitoring of methotrexate as clinical decision support for personalized medicine: a brief review, Biomed. Chromatogr. 32 (5) (2018), e4159.
[8] B.C. Widemann, P.C. Adamson, Understanding and managing methotrexate nephrotoxicity, oncologist 11 (6) (2006) 694–703.
[9] A.F. Hawwa, A. AlBawab, M. Rooney, L.R. Wedderburn, M.W. Beresford, J. C. McElnay, Therapy, Methotrexate polyglutamates as a potential marker of adherence to long-term therapy in children with juvenile idiopathic arthritis and juvenile dermatomyositis: an observational, cross-sectional study, Arthritis Res 17 (2015) 1–10.
[10] M. Stachowiak, M. Cegłowski, J. Kurczewska, Hybrid chitosan/molecularly imprinted polymer hydrogel beads doped with iron for selective ibuprofen adsorption, Int. J. Biol. Macromol. 251 (2023), 126356.
[11] X. Cao, Y. Hu, H. Yu, S. Sun, D. Xu, Z. Zhang, S. Cong, Y. She, Detection of neonicotinoids in agricultural products using magnetic molecularly imprinted polymers-surface enhanced Raman spectroscopy, Talanta 266 (2024), 125000.
[12] Y. Hu, T. Liu, S. Wang, M. Lv, Y. She, B. Cao, Z. Zhang, X. Cao, Preparation of magnetic molecularly imprinted polymers for the selective extraction of strobilurin fungicides in agricultural products, J. Food Compos. Anal. 123 (2023), 105564.
[13] S. Wang, L. Zhang, J. Zeng, X. Hu, X. Wang, L. Yu, D. Wang, L. Cheng, R. Ahmed, V. Romanovski, P. Li, Z. Zhang, Multi-templates molecularly imprinted polymers for simultaneous recognition of multiple targets: From academy to application, TrAC, Trends Anal. Chem. 166 (2023), 117173.
[14] N. Azizi-Khereshki, H.Z. Mousavi, M.G. Dogaheh, M. Farsadrooh, N. Alizadeh, A. Mohammadi, Synthesis of molecularly imprinted polymer as a nanosorbent for dispersive magnetic micro solid-phase extraction and determination of valsartan in biological samples by UV–Vis Spectrophotometry: Isotherm, kinetics, and thermodynamic studies, Spectrochim. Acta A 296 (2023), 122656.
[15] J. Tang, Y. Ren, L. Zhu, Y. Chen, S. Liu, L. Zhu, R. Yang, Magnetic molecularly imprinted polymer combined with solid-phase extraction for detection of kojic acid in cosmetic products, Microchem. J. 183 (2022), 108028.
[16] T. Zhou, Z. Deng, Q. Wang, H. Li, S. Li, X. Xu, Y. Zhou, S. Sun, C. Xuan, Q. Tian, L. Lun, Magnetic Molecularly Imprinted Polymers for the Rapid and Selective Extraction and Detection of Methotrexatein Serum by HPLC-UV Analysis, molecules 27 (18) (2022) 6084.
[17] R. Khalifeh, M. Ghamari, A multicomponent synthesis of 2-amino-3-cyanopyridine derivatives catalyzed by heterogeneous and recyclable copper nanoparticles on charcoal, J. Braz. Chem. Soc. 27 (2016) 759–768.
[18] A. Vibhute, T. Patil, D. Malavekar, S. Patil, S. Lee, A.P. Tiwari, Green synthesis of fluorescent carbon dots from annona squamosa leaves: optical and structural properties with bactericidal, anti-inflammatory, anti-angiogenesis applications, J. Fluoresc. 33 (4) (2023) 1619–1629.
[19] S.A. Alkahtani, A.M. Mahmoud, Y.S. Alqahtani, A.-M.B.H. Ali, M.M. El-Wekil, Selective detection of rutin at novel pyridinic-nitrogen-rich carbon dots derived from chicken feet biowaste: The role of bovine serum albumin during the assay, Spectrochim. Acta A 303 (2023), 123252.
[20] A.M. Mahmoud, S.S. Abu-Alrub, A.O. Alqarni, M.M. El-Wekil, A.-M.B.H. Ali, Convenient electrochemical and fluorometric dual-mode estimation of diosmin using carbon dots doped with nitrogen derived from chicken feet biowaste, Microchem. J. 191 (2023), 108929.
[21] Sumaiyah, P.A.Z. Hasibuan, M. Tanjung, W. Lianto, S. Gea, A. Piliang, S.A. Situmorang, Hydrothermally nitrogen-doped carbon dots (N-C-dots) from isolated lignin of oil palm empty fruit bunch for bacterial imaging of Staphylococcus aureus, Case Stud. Chem. Environ. Eng. 8 (2023) 100455.
[22] R. Sangubotla, J. Kim, Ultra-sensitive turn-on fluorescent sensor based on β-cyclodextrin-stabilized melamine-derived carbon dots for the highly selective dual-detection of dopamine, Ceram. Int. 49 (10) (2023) 16272–16282.
[23] S. Gao, H. Zhang, H. Li, Y. Pei, Synthesis of sulfur-chlorine-doped fluorescent carbon quantum dots from leachate membrane concentrate as a selective probe for Pd^{2+} detection, Opt. Mater. 139 (2023), 113746.
[24] X. Ma, R. Sun, J. Cheng, J. Liu, F. Gou, H. Xiang, X. Zhou, Fluorescence aggregation-caused quenching versus aggregation-induced emission: a visual teaching technology for undergraduate chemistry students, J. Chem. Educ. 93 (2) (2016) 345–350.
[25] W. Wang, Y.-C. Lu, H. Huang, A.-J. Wang, J.-R. Chen, J.-J. Feng, Facile synthesis of N, S-codoped fluorescent carbon nanodots for fluorescent resonance energy transfer recognition of methotrexate with high sensitivity and selectivity, Biosens. Bioelectron. 64 (2015) 517–522.
[26] Z. Chen, S. Qian, X. Chen, W. Gao, Y. Lin, Protein-templated gold nanoclusters as fluorescence probes for the detection of methotrexate, Analyst 137 (18) (2012) 4356–4361.
[27] Y. Zhao, S. Zou, D. Huo, C. Hou, M. Yang, J. Li, M. Bian, Simple and sensitive fluorescence sensor for methotrexate detection based on the inner filter effect of N, S co-doped carbon quantum dots, Anal. Chim. Acta 1047 (2019) 179–187.
[28] M. Molaparast, P. Eslampour, J. Soleymani, V. Shafiei-Irannejad, Spectrofluorimetric method for monitoring methotrexate in patients' plasma samples and cell lysates using highly fluorescent carbon dots, J. Pharm. Innov. 21 (1) (2022), e126918.
[29] P. Zuo, J. Liu, H. Guo, C. Wang, H. Liu, Z. Zhang, Q. Liu, Multifunctional N,S co-doped carbon dots for sensitive probing of temperature, ferric ion, and methotrexate, Anal. Bioanal. Chem. 411 (8) (2019) 1647–1657.
[30] A. Jouyban, M. Shaghaghi, L.M. J, J. Soleymani, J. Jalilvaez-Gharamaleki, Determination of methotrexate in biological fluids and a parenteral injection using terbium-sensitized method, Iran, J. Pharm. Sci.: IJPR 10 (4) (2011) 695–704.
[31] A. Mohammadzadeh, A. Jouyban, M. Hasanzadeh, V. Shafiei-Irannejad, J. Soleymani, Ultrasensitive fluorescence detection of antitumor drug methotrexate based on a terbium-doped silica dendritic probe, Anal. Methods 13 (37) (2021) 4280–4289.
[32] Z. Golsanamlou, H. Kholafazad-Kordasht, J. Soleymani, A. Jouyban, Quantification of methotrexate in plasma samples using highly fluorescent nanoparticles, J. Pharm. Biomed. Anal. 214 (2022), 114716.
[33] H. Hamishehkar, B. Ghasemzadeh, A. Naseri, R. Salehi, F. Rasoulzadeh, Carbon dots preparation as a fluorescent sensing platform for highly efficient detection of Fe (III) ions in biological systems, Spectrochim. Acta A. 150 (2015) 934–939.
[34] W. Gu, X. Pei, Y. Cheng, C. Zhang, J. Zhang, Y. Yan, C. Ding, Y. Xian, Black phosphorus quantum dots as the ratiometric fluorescence probe for trace mercury ion detection based on inner filter effect, ACS Sens. 2 (4) (2017) 576–582.
[35] J. Wang, Q. Shen, X. Yu, Q. Kang, D. Shen, A smartphone-based ratiometric fluorescence and absorbance dual-mode device for Rhodamine B determination in combination with differential molecularly imprinting strategy and primary inner filter effect correction, Microchem. J. 183 (2022), 108077.